

NEUTRON SOURCES IN EARLY STARS*

MICHAEL WIESCHER, RICHARD J. DEBOER, JOACHIM GÖRRES
AUGUST GULA, QIAN LIU

University of Notre Dame
Department of Physics and the Joint Institute for Nuclear Astrophysics
Notre Dame, IN 46556, USA

(Received January 7, 2020)

Stellar abundance distributions in carbon enhanced metal poor carbon stars strongly suggest the existence of a third neutron-induced nucleosynthesis process beyond the s- and the r-processes, facilitating the build-up of elements in early star generations. This process is called the intermediate or i-process and is proposed to take place in a very dynamic stellar environment, driven by fast mixing and deep convection. This paper will summarize our understanding of neutron sources in stars and the sensitive role of macroscopic dynamics in the stellar environment, and the microscopic structure of the associated nuclei before discussing possible neutron sources that may emerge in an early or primordial stellar environment. It will present the current status of the experimental knowledge and the limits of the theoretical interpretation of the associated reaction rates.

DOI:10.5506/APhysPolB.51.631

1. Introduction

The production of heavy elements beyond iron is traditionally associated with the slow (s) [1] and rapid (r) [2] neutron-capture processes. The s-process is characterized by a relatively low neutron flux, and its reaction path is a sequence of neutron captures and β -decays along the line of stability. The r-process, on the other hand, occurs at high neutron flux, with a reaction path along the very neutron rich side of stability. A high neutron flux is expected in explosive environments such as type II core collapse supernova or neutron star mergers. This paper will concentrate on neutron-induced processes which rely on nuclear reaction driven (α, n) neutron sources. The efficiency of these sources typically depends on a complex

* Presented at the XXXVI Mazurian Lakes Conference on Physics, Piaski, Poland, September 1–7, 2019.

interplay between the macroscopic dynamics in the stellar environment, the charged particle reactions that produce the isotopic seed material for these sources and the nuclear structure that determines the (α, n) reaction rate. In the following, we will provide a short description of the environmental conditions for the production of neutrons in different stellar environments, followed by a discussion of the underlying microscopic issues of threshold resonances enhancing the (α, n) reaction rates.

2. Neutron sources in stellar environments

Two components have been identified for the s-process, the weak s-process in the helium burning core of massive red giant stars, and the main s-process in the helium burning shell of low mass AGB stars. The main neutron source for the weak s-process is the $^{22}\text{Ne}(\alpha, n)^{25}\text{Mg}$ reaction, with ^{22}Ne being produced from the ^{14}N ashes of the preceding CNO hydrogen burning.

The neutron source for the main s-process is the $^{13}\text{C}(\alpha, n)^{16}\text{O}$ reaction in the helium burning shell of AGB stars, which contains an appreciable amount of ^{12}C being produced by the triple-alpha process. Convective mixing of hydrogen into the shell, triggers the reaction sequence $^{12}\text{C}(p, \gamma)^{13}\text{N}(\beta^+ \nu)^{13}\text{C}$, the amount of mixed-in hydrogen determines the intensity of the neutron flux. It is an environmentally sensitive process [3], a balance between temperature and proton infusion, which needs sophisticated dynamic model treatment for evaluating its full impact [4].

There have been a number of other processes proposed, which might generate an intensive enough neutron flux to translate into a reaction path along the neutron rich side of the line of stability. The two best known processes are the intermediate (i) process [5] and the n-process [6, 7]. Both rely on the same concept as the s-process but require a highly dynamic component in the stellar environment to substantially increase the neutron flux.

The i-process considers the special case of a deep convective environment in the helium burning zone in which the freshly produced ^{13}N is rapidly mixed to its hot bottom within a timescale comparable with the decay time of the nucleus. The $^{13}\text{C}(\alpha, n)^{16}\text{O}$ reaction ignites at a much higher temperature providing a much higher neutron flux up to 10^{16} neutrons/cm⁻³ [8]. This process takes place in massive AGB stars and the characteristic abundance distribution is observed in early stars, so-called CEMP stars [4].

The n-process is based on the conditions in a helium burning shell of a massive pre-supernova star being rapidly modified by the passage of the supernova shock front. Material is compressed and temperature and density quickly reach a maximum, followed by an expansion where they decrease

rapidly on a timescale of a second [9]. The high peak temperature causes an efficient activation of the $^{22}\text{Ne}(\alpha, n)^{25}\text{Mg}$ reaction, which triggers a neutron burst with neutron density peaks up to 10^{18} neutrons/cm $^{-3}$ or higher. This process does not produce the characteristic r-process features but changes the abundance structure of medium mass elements as reflected in meteoritic inclusions [10].

The strength of the two reactions $^{13}\text{C}(\alpha, n)^{16}\text{O}$ and $^{22}\text{Ne}(\alpha, n)^{25}\text{Mg}$ depends critically on the nuclear structure at the α threshold in the compound nuclei ^{17}O and ^{26}Mg , respectively. In both cases, α clustering seems to cause resonance structures that enhance the stellar reaction rates. The purpose of the here presented work is to explore the possibility of other cases where near threshold resonance configurations could emerge as neutron sources in specific stellar environments. In the following chapter, we present a more detailed discussion on the $^{13}\text{C}(\alpha, n)^{16}\text{O}$ and $^{22}\text{Ne}(\alpha, n)^{25}\text{Mg}$ cases before introducing a new possibility for neutron sources in very early, population III stellar environments [11, 12].

3. Threshold resonances in the $^{13}\text{C}+\alpha$ system

Earlier experimental studies of the $^{13}\text{C}(\alpha, n)^{16}\text{O}$ reaction [13] seem to confirm a previously observed up-swing in the S -factor of the reaction at very low energies [14], but the data are certainly handicapped by strong neutron background. If confirmed in present underground experiments, this up-swing could be the tail of a previously observed broad near-threshold resonance at $E_\alpha = -3$ keV with a total width of $\Gamma_{\text{total}} = \Gamma_n = 124 \pm 12$ keV [15, 16]. A recent transfer reaction study suggested a slightly higher energy and width, $E_\alpha = +4.7 \pm 3$ keV and $\Gamma_{\text{total}} = \Gamma_n = 136 \pm 5$ keV [12].

Several experiments have been performed to probe the α strength of this level using a variety of α -transfer reaction techniques, including the so-called Trojan Horse Technique (THM) [17–20]. The α strength determines the resonance strength in the $^{13}\text{C}(\alpha, n)^{16}\text{O}$ reaction. The experiments provide a broad range of differing results for the spectroscopic α factor $S_\alpha = 0.01$ to 0.037 ± 0.12 [20]. The higher values would indeed suggest a pronounced threshold resonance that would considerably enhance the reaction rate at low temperatures, but the close proximity of the $1/2^+$ state to threshold means that the ANCs are very sensitive to the resonance energy [21]. The large uncertainty in energy may transfer into a very large uncertainty in contribution to the cross section of this low-energy resonance when implemented in an R-matrix formalism.

One earlier study [22] used ANC data to calculate the impact on the S -factor of the reaction. Taking into account the large range of uncertainty in the resonance energy and other parameters, we performed a new R-matrix

analysis using the code AZURE2 [23, 24] to evaluate the impact of the resonance energy, width, and α strength on the S -factor of the $^{13}\text{C}(\alpha, n)^{16}\text{O}$ reaction. Figure 1 compares one calculation of the S -factor curve with the lowest energy experimental data [13, 14]. Here, the Coulomb modified ANC from Ref. [20] has been used. The results indicate an S -factor that is below the central value of the lowest energy data points, but is still within the experimental uncertainties. More reliable, α -capture studies are needed in an underground accelerator environment with reduced neutron background [25] such as LUNA and CASPAR to reduce the uncertainties at low energy and test the R-matrix predictions presented here. First studies at the LNGS accelerator LUNA indicate that the rise in S -factor is less pronounced than suggested by earlier experiments. If confirmed, this could translate into a lower α strength, as also indicated in the here presented R-matrix fit (see Fig. 1).

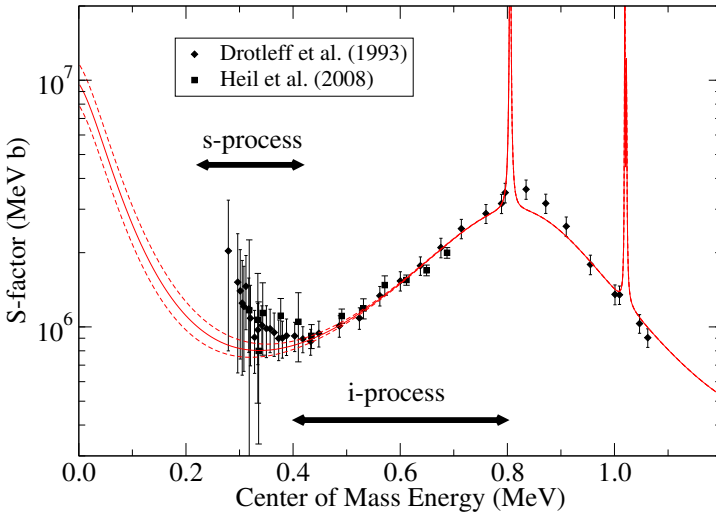


Fig. 1. R-matrix calculation of the low-energy S -factor of the $^{13}\text{C}(\alpha, n)^{16}\text{O}$ reaction compared to the experimental data of Refs. [13, 14]. The Gamow energy ranges for the s- and i-processes are indicated by the arrows.

4. Threshold resonances in the $^{22}\text{Ne}+\alpha$ system

While the impact of the $^{13}\text{C}(\alpha, n)^{16}\text{O}$ threshold resonance remains uncertain, a clearer picture can be presented for the case of the $^{22}\text{Ne}(\alpha, n)^{25}\text{Mg}$ neutron source. The reaction rate is dominated by a single resonance at $E_{\text{cm}} = 703 \pm 2$ keV, corresponding to a state at 11.32 MeV excitation energy. The level is observed in both the $^{22}\text{Ne}(\alpha, n)^{25}\text{Mg}$ [26] and the $^{22}\text{Ne}(\alpha, \gamma)^{26}\text{Mg}$ [27] reaction channels. It is also strongly observed in α -trans-

fer studies [28], but not observed in the $^{25}\text{Mg}(n, \gamma)^{26}\text{Mg}$ reaction [29, 30] and is only weakly populated in the $^{25}\text{Mg}(d, p)^{26}\text{Mg}$ neutron-transfer reaction. The present experimental results indicate a pronounced α cluster configuration with negligible single-particle strength. The lower energy range of the $^{22}\text{Ne}+\alpha$ reactions has not yet been explored with sufficient accuracy to identify other cluster states closer to the threshold, which will impact the ratio of the (α, γ) and (α, n) reaction rates [31]. However, the transfer studies indicate the possibility of such levels. Again considerable efforts are being undertaken to probe these reactions at the LUNA and CASPAR underground accelerator laboratories. Figure 2 shows an R-matrix calculation for the $^{22}\text{Ne}(\alpha, n)^{25}\text{Mg}$ cross section that was performed on the basis of the presently available data, including results from transfer and $^{25}\text{Mg}+n$ measurements in order to estimate the cross section at very low energies. Based on these predictions, it is expected that the yet unobserved low-energy resonances of the $^{22}\text{Ne}(\alpha, n)^{25}\text{Mg}$ reaction can be directly investigated.

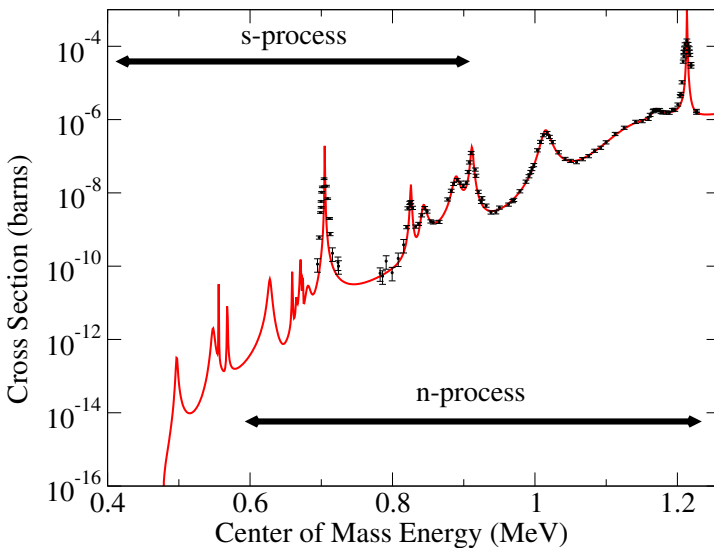


Fig. 2. R-matrix fit to the $^{22}\text{Ne}(\alpha, n)^{25}\text{Mg}$ cross section data of Ref. [26]. At lower energies, an estimate of the cross section is made based on transfer and $^{25}\text{Mg}+n$ measurements. The arrows indicate the Gamow range of energy for the s- and n-processes.

5. Neutron sources in first stars?

The previous examples highlighted the importance of α -cluster states near the threshold for the efficiency of stellar neutron sources, an efficiency that may be further enhanced by the dynamics in the stellar environment.

Yet, both sources $^{13}\text{C}(\alpha, n)^{16}\text{O}$ and $^{22}\text{Ne}(\alpha, n)^{25}\text{Mg}$ rely on specific mechanisms that provide a sufficient amount of ^{13}C and ^{22}Ne seed material. Besides the reaction strength, these mechanisms represent an important aspect for all neutron sources.

There are multiple other neutron sources such as the $^9\text{Be}(\alpha, n)^{12}\text{C}$, $^{10}\text{B}(\alpha, n)^{13}\text{N}$, and $^{11}\text{B}(\alpha, n)^{14}\text{N}$ reactions, which could in principle serve as strong neutron sources if sufficient abundance of seed elements can be provided. These high cross sections are due to the α -cluster structure of target and compound nuclei ^{13}C , ^{14}N , and ^{15}N , respectively. Cluster states above the α threshold facilitate a strong reaction probability. The cluster nature of ^{13}C as a $1n \otimes 3\alpha$ configuration was recently theoretically confirmed [32]. Similar configurations are anticipated for ^9Be ($1n \otimes 2\alpha$), ^{17}O ($1n \otimes 4\alpha$), ^{21}Ne ($1n \otimes 5\alpha$) *etc.* This suggests strong α -transition strengths between these nuclei. This, coupled with the high probability for removal of the single-valence neutron, drives the strength of the respective (α, n) cross sections, including the $^9\text{Be}(\alpha, n)^{12}\text{C}$ and $^{13}\text{C}(\alpha, n)^{16}\text{O}$ reactions, but also the $^{10}\text{B}(\alpha, n)^{13}\text{N}$, which is built on a threshold cluster state in the compound nucleus ^{14}N . Target and compound configurations are characterized by a $(1d \otimes 2\alpha)$ and $(1d \otimes 3\alpha)$ structure, respectively. Such configurations could facilitate threshold resonances and enhance the overall strength of these reactions in a primordial stellar burning environment.

First stars burn on their primordial abundance distribution generated by Big Bang nucleosynthesis. Model simulations of first stars indicate a mass distribution ranging from $5 M_{\odot}$ to $150 M_{\odot}$ [33]. Because of the absence of carbon, the CNO cycles cannot contribute to the energy production to stabilize the star against gravitational contraction. Because the *pp*-chains are not an efficient energy source for stabilizing the star, the core gradually contracts, following the Helmholtz–Kelvin time-scale, reaching conditions where alternative reaction branches may trigger the hot *pp*-chains [34]. Recent simulations of nucleosynthesis in primordial stars indicate the possibility of additional reaction chains, which are driven by α -capture reactions in a strong hydrogen burning environment [11]. One of the reaction branches is triggered by the $^2\text{H}(\alpha, \gamma)^6\text{Li}$ radiative capture process [35] on the highly abundant deuterium content in primordial matter. The subsequent $^6\text{Li}(\alpha, \gamma)^{10}\text{B}$ reaction competes with the strong $^6\text{Li}(p, \alpha)^3\text{He}$ reaction [36] (as shown in Fig. 3), which reprocesses material back to helium, and in turn will be available for further processing. The subsequent α -capture reaction on ^{10}B also competes with strong proton-induced reactions such as $^{10}\text{B}(p, \alpha)^7\text{Be}$ [37]. The former has been shown in this work to be many orders of magnitude stronger than earlier estimates [38] (see Fig. 3). Alpha capture on ^{10}B populates the compound nucleus ^{14}N at high excitation energies, several exit channels are open allowing for the $^{10}\text{B}(\alpha, p)^{13}\text{C}$, $^{10}\text{B}(\alpha, d)^{12}\text{C}$, and $^{10}\text{B}(\alpha, n)^{13}\text{N}$ reactions to proceed.

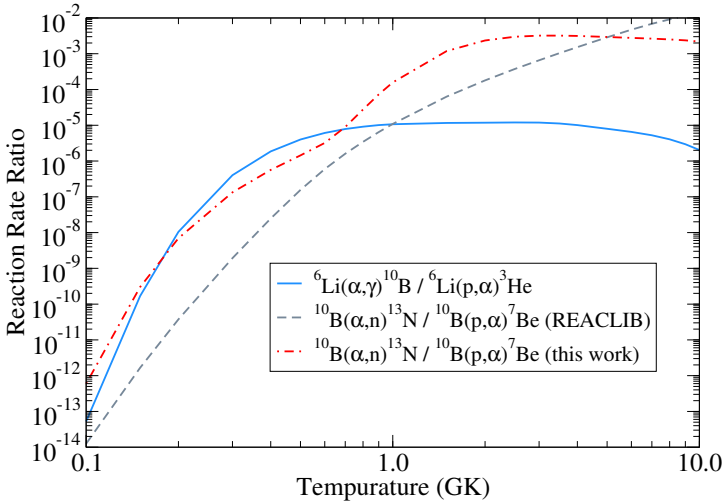


Fig. 3. Ratio of the ${}^6\text{Li}(\alpha, \gamma){}^{10}\text{B}$ reaction rate to the competing ${}^6\text{Li}(p, \alpha){}^3\text{He}$ reaction rate and ratio of ${}^{10}\text{B}(\alpha, n){}^{13}\text{N}$ reaction rate to the competing ${}^{10}\text{B}(p, \alpha){}^7\text{Be}$ reaction rate. Rates taken from JINA REACLIB [39], except for the ${}^{10}\text{B}(\alpha, n){}^{13}\text{N}$ reaction rate that is based on new measurements at the University of Notre Dame.

We have performed a number of experiments at the Nuclear Science Laboratory of the University of Notre Dame, which clearly show a pronounced increase in the low-energy S -factor in all three reaction channels, suggesting a pronounced α cluster structure just above the α threshold in ${}^{14}\text{N}$. Tentatively, we assign this cluster state to the level in ${}^{14}\text{N}$ that has been detected in yet unpublished high-resolution ${}^{10}\text{B}({}^6\text{Li}, d){}^{14}\text{N}$ α -transfer study at $E_x = 11.956(5)$ MeV [40]. Angular distribution analysis suggests a spin parity assignment of $J^\pi = 2^-$. This could indeed be one of the near threshold cluster configurations like those observed in the ${}^{13}\text{C}(\alpha, n){}^{16}\text{O}$ and ${}^{22}\text{Ne}(\alpha, n){}^{25}\text{Mg}$ reactions. Figure 4 shows the results of a comprehensive R-matrix fit taking all three reaction channels into account. One can clearly recognize the tail in the experimental data which can be fit by a broad resonance. Similar to the case of the ${}^{13}\text{C}(\alpha, n){}^{16}\text{O}$ and ${}^{22}\text{Ne}(\alpha, n){}^{25}\text{Mg}$ reactions, this low-energy resonance has a large α strength with weak single particle strengths for the proton and neutron channels.

While the experimental data have not been pushed far enough into the lower energy range to confirm a resonance shape in the S -factor, the existence of such a resonance might have a significant impact on first star nucleosynthesis patterns. The overall strength of the ${}^{10}\text{B}+\alpha$ reaction rates is being strengthened by several orders of magnitude compared to the ${}^{10}\text{B}+p$ branch. The ${}^{10}\text{B}(\alpha, p){}^{13}\text{C}$ reaction would generate a strong link, feeding ${}^{13}\text{C}$ and, therefore, help to create a potential CNO cycle environment. Likewise

the $^{10}\text{B}(\alpha, d)^{12}\text{C}$ reaction would add to the CNO seed nuclei but would also feed deuterons back into the environment as new seed nuclei for a cyclic deuterium-induced reaction pattern, which will fuel the here discussed reaction sequence. Finally, the $^{10}\text{B}(\alpha, n)^{13}\text{N}$ reaction would generate a neutron flux in the early stellar environment. The reaction acts as a neutron source but to determine its efficiency, more detailed simulations are necessary to understand the complexity of the nucleosynthesis process in a highly convective first star environment taking into account a range of possibilities for H–He interactions between the H- and He-convection zones [41].

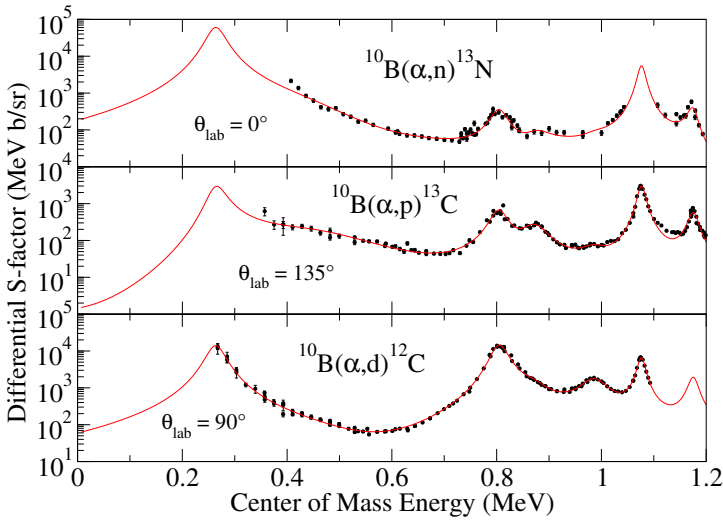


Fig. 4. (Color online) Preliminary low-energy data for the $^{10}\text{B}(\alpha, n)^{13}\text{N}$, $^{10}\text{B}(\alpha, p)^{13}\text{C}$, and $^{10}\text{B}(\alpha, d)^{12}\text{C}$ reactions. The solid red line indicates a simultaneous R-matrix fit.

6. Outlook

The here discussed cases of near-threshold cluster resonances in stellar neutron sources are only a few examples for the impact of cluster configurations in nuclear astrophysics [42]. The existence of such cluster configurations near the thresholds have been, in many cases, observed and explained phenomenologically in the framework of the Ikeda rule [43]. However, only recently, a theoretical explanation has been proposed to microscopically explain the appearance of such structures in close vicinity to threshold as a consequence of an openness of the nuclear many-body system, which leads to the collectivization of Shell Model (SM) states into cluster configurations [44]. This model demonstrates that the cluster configurations emerge fairly independent of the structure of the respective compound nucleus. This

approach, the Shell Model Embedded in the Continuum (SMEC), provides a unified description of structure and reactions with up to two nucleons in the scattering continuum using realistic SM interactions. This theory has been successfully applied to cases such as the cluster states facilitating the triple-alpha-process [45]. A better theoretical basis for the here discussed role of cluster states in stellar neutron sources would be more than desirable.

REFERENCES

- [1] F. Käppeler, R. Gallino, S. Bisterzo, W. Aoki, *Rev. Mod. Phys.* **83**, 157 (2011).
- [2] M.R. Mumpower, R. Surman, G.C. McLaughlin, A. Aprahamian, *Prog. Part. Nucl. Phys.* **86**, 86 (2016).
- [3] S. Cristallo *et al.*, *Astrophys. J.* **859**, 105 (2018).
- [4] S. Bisterzo *et al.*, *Astrophys. J.* **787**, 10 (2014).
- [5] J.J. Cowan, W.K. Rose, *Astrophys. J.* **212**, 149 (1977).
- [6] J.B. Blake, D.N. Schramm, *Astrophys. J.* **209**, 846 (1976).
- [7] J.W. Truran, J.J. Cowan, A.G.W. Cameron, *Astrophys. J. Lett.* **222**, L63 (1978).
- [8] S. Jones *et al.*, *Mon. Not. R. Astron. Soc.* **445**, 3848 (2015).
- [9] A. Heger, S.E. Woosley, *Astrophys. J.* **567**, 532 (2002).
- [10] M. Pignatari *et al.*, *Geochim. Cosmochim. Acta* **221**, 37 (2018).
- [11] O. Clarkson, F. Herwig, M. Pignatari, *Mon. Not. R. Astron. Soc. Lett.* **474**, L37 (2017).
- [12] T. Faestermann, P. Mohr, R. Hertenberger, H.-F. Wirth, *Phys. Rev. C* **92**, 052802 (2015).
- [13] M. Heil *et al.*, *Phys. Rev. C* **78**, 025803 (2008).
- [14] H.W. Drotleff, *et al.*, *Astrophys. J.* **414**, 735 (1993).
- [15] J.L. Fowler, C.H. Johnson, *Phys. Rev. C* **2**, 124 (1970).
- [16] C.H. Johnson, *Phys. Rev. C* **7**, 561 (1973).
- [17] S. Kubono *et al.*, *Phys. Rev. Lett.* **90**, 062501 (2003).
- [18] N. Keeley, K.W. Kemper, D.T. Khoa, *Nucl. Phys. A* **726**, 159 (2003).
- [19] M. La Cognata *et al.*, *Astrophys. J.* **777**, 143 (2013).
- [20] M.L. Avila *et al.*, *Phys. Rev. C* **91**, 048801 (2015).
- [21] N. Keeley, K.W. Kemper, K. Rusek, *Eur. Phys. J. A* **54**, 71 (2018).
- [22] E.D. Johnson *et al.*, *Phys. Rev. Lett.* **97**, 192701 (2006).
- [23] R.E. Azuma *et al.*, *Phys. Rev. C* **81**, 045805 (2010).
- [24] R.J. deBoer *et al.*, *Rev. Mod. Phys.* **89**, 035007 (2017).
- [25] A. Best *et al.*, *Nucl. Instrum. Methods Phys. Res. A* **812**, 1 (2016).

- [26] M. Jaeger *et al.*, *Phys. Rev. Lett.* **87**, 202501 (2001).
- [27] K. Wolke *et al.*, *Z. Phys. A* **334**, 491 (1989).
- [28] R. Talwar *et al.*, *Phys. Rev. C* **93**, 055803 (2016).
- [29] C. Massimi *et al.*, *Phys. Rev. C* **85**, 044615 (2012).
- [30] C. Massimi *et al.*, *Phys. Lett. B* **768**, 1 (2017).
- [31] F. Käppeler *et al.*, *Astrophys. J.* **437**, 396 (1994).
- [32] R. Bijker, F. Iachello, *Phys. Rev. Lett.* **122**, 162501 (2019).
- [33] V. Bromm, N. Yoshida, L. Hernquist, C.F. McKee, *Nature* **459**, 49 (2009).
- [34] M. Wiescher *et al.*, *Astrophys. J.* **343**, 352 (1989).
- [35] D. Trezzi *et al.*, *Astropart. Phys.* **89**, 57 (2017).
- [36] L. Lamia *et al.*, *Astrophys. J.* **768**, 65 (2013).
- [37] M. Wiescher, R.J. deBoer, J. Görres, R.E. Azuma, *Phys. Rev. C* **95**, 044617 (2017).
- [38] G.R. Caughlan, W.A. Fowler, *At. Data Nucl. Data Tables* **40**, 283 (1988).
- [39] R.H. Cyburt *et al.*, *Astrophys. J. Suppl. Ser.* **189**, 240 (2010).
- [40] H.T. Fortune, private communication.
- [41] O. Clarkson *et al.*, *Nuclei in the Cosmos XV*, Springer Proceedings in Physics, 2019, p. 321, https://doi.org/10.1007/978-3-030-13876-9_56 [[arXiv:1810.12259](https://arxiv.org/abs/1810.12259) [astro-ph.SR]].
- [42] M. Wiescher, T. Ahn, *Clusters in Astrophysics in: Nuclear Particle Correlations Cluster Physics*, World Scientific, 2017, pp. 203–255.
- [43] K. Ikeda, T. Marumori, R. Tamagaki, H. Tanaka, *Prog. Theor. Phys. Suppl.* **52**, 1 (1972).
- [44] J. Okołowicz, M. Płoszajczak, W. Nazarewicz, *Prog. Theor. Phys. Suppl.* **196**, 230 (2012).
- [45] J. Okołowicz, W. Nazarewicz, M. Płoszajczak, *Fortschr. Phys.* **61**, 66 (2013).